Protoplasma 111, 134–150 (1982)

PROTOPLASMA

Intercellular Communication in *Azolla* Roots: I. Ultrastructure of Plasmodesmata

R. L. Overall[1,*], J. Wolfe[2], and B. E. S. Gunning[1]

[1] Department of Developmental Biology, Research School of Biological Sciences, Australian National University, Canberra City, Australia
[2] Division of Plant Industry, CSIRO, Canberra City, Australia

Received November 15, 1981
Accepted December 15, 1981

Summary

A model is proposed for the structure of the plasmodesmata of *Azolla* root primordia, based on micrographs obtained by a combination of fixation in glutaraldehyde/p-formaldehyde/tannic acid/ferric chloride, digestion of cell walls and the use of stereo pairs. Unlike the model for plasmodesmatal structure proposed by Robards (1971), the desmotubule is depicted as a virtually closed cylindrical bilayer providing little or no open pathway for transport. In this respect it is similar to the model of López-Sáez *et al.* (1966). An analysis of the molecular packing of types of lipids found in endoplasmic reticulum (of which the desmotubule is an extension) indicates that the model is geometrically feasible. Details cannot be discerned with accuracy, but material, possibly particulate, occupies much of the space between desmotubule and plasma membrane, the cytoplasmic lumen being reduced to inter-particle spaces of cross-sectional area comparable to that of the bore in a gap junction connexon. Implications for intercellular transport are discussed.

Keywords: Azolla; plasmodesmata; desmotubule; membrane; intercellular communication.

1. Introduction

The current, and widely-accepted, model of plasmodesmatal ultrastructure (reviewed by Robards 1976, Gunning and Robards 1976) offers two possible pathways for cell-to-cell transport. One is the "desmotubule", a derivative of endoplasmic reticulum (ER) which passes from cell to cell along the axis of the plasmodesma. The other is the "cytoplasmic annulus" lying between the desmotubule and the plasma membrane that delimits the plasmodesma.

No electrophysiological or other studies to date answer the question of which pathway(s) might be utilised in the plant. The cells and tissues that have been examined in terms of function have not been subjected to ultrastructural examination at high-resolution. The cytoplasmic annulus is often constricted at its orifices but is a potential route for exchanging cytosolic molecules. The desmotubule, if its lumen is indeed open, is part of an extra-cytosolic compartment, protected by the membrane of the ER. Together, the two pathways could, in theory, cope with different categories of mobile molecules, and even with two opposing directions of transport. If true, this would represent a level of complexity not attained in animal tissues (Loewenstein *et al.* 1978). The questions raised are fundamental to an understanding of the nature and role of symplastic intercellular communication in plants, hence it is very desirable to come to a conclusion regarding the realities of structure and function in plasmodesmata.

Observations presented here support the view of López-Sáez *et al.* (1966) that the axial structure of plasmodesmata is not an open tubule, although it is attached at both ends to ER. Further, the cytoplasmic annulus is partially occluded, to the extent that the pathway for transport may be of comparable cross-sectional area to that seen in gap junctions in animals.

* Correspondence and Reprints: Department of Biological Sciences, Lilly Hall of Life Sciences, Purdue University, West Lafayette, IN 47907, U.S.A.

0033-183X/82/0111/0134/$ 03.40

2. Materials and Methods

Roots less than 0.5 mm in length were dissected from *Azolla pinnata* R. Br. cultured on growth medium: 0.2 mM KH_2PO_4, 0.4 mM $CaCl_2$, 0.3 mM $MgSO_4$, 0.25 mM K_2SO_4, 0.1 mM NaCl plus micronutrients (W. RAINS, pers. comm.).

Standard preparations were fixed in 2.5% glutaraldehyde plus 2% p-formaldehyde (glut/p-form) in 0.025 M phosphate buffer (pH 6.8) for 2 hours at room temperature, rinsed in several changes of buffer; post-fixed in 2% osmium tetroxide in the same buffer for 1 hour at room temperature; dehydrated in graded acetone solutions; embedded in Epoxy resin (SPURR 1969) and sectioned for electron microscopy. In other preparations, 2% tannic acid (Mallinckrodt 1764, Mallinckrodt Chemical Works, St. Louis) was added to the conventional glut/p-form primary fixative above. After 2 hours at room temperature the tissue was rinsed in several changes of distilled water, treated in 2% $FeCl_3$ (NEHLS and SCHAFFNER 1976, LA FOUNTAIN *et al.* 1977) in distilled water for 2 hours, rinsed briefly and dehydrated and embedded as above (glut/p-form/tannic acid/$FeCl_3$).

To remove cell wall material, some roots were left in 2% driselase (Kyowa-Hakko-Kogya, Tokyo, Japan) plus 1% chloramphenicol for 2 or 6 hours after the ferric chloride treatment, before dehydration and embedding.

Suspensions of isolated walls were prepared by macerating conventionally or tannic acid/$FeCl_3$-fixed roots in a mortar and pestle in phosphate buffer or distilled water respectively. Suspension were centrifuged successively during dehydration steps, embedded, pelleted, and polymerised in "Beem" capsules before sectioning.

Grids bearing unsupported sections were stained with 5% uranyl acetate in 50% ethanol, followed by lead citrate (REYNOLDS 1963), and examined using an Hitachi H 600 electron microscope. Stereo pairs of plasmodesmata were obtained by photographing at 5° intervals through the range $-20°$ to $+20°$ using the side entry goniometer stage.

Dimensions are expressed as means ± standard deviations, followed (in brackets) by the number of observations. Measurements were made on negatives to reduce problems of variation in the apparent position of boundary edges with changes in print contrast. Although the data have been averaged and expressed to the nearest 0.1 nm in order that comparisons with theoretical values can be made, the averages so obtained do not imply that the level of precision was attained – merely that the quoted values have the best available probability of being accurate.

3. Results

3.1. General Preservation

Images yielded by the glut/p-form/tannic acid/$FeCl_3$ procedure (Figs. 1–6) accord well with previous experience of cells in *Azolla* root primordia (*e.g.*, GUNNING *et al.* 1978). However, membranes are delineated with unusual clarity, their outer faces staining darkly and contrasting with the electron-lucent interior. Where present, dense material along a face of a membrane is readily seen. The procedure was developed for enhancing visibility of filamentous material in sections (FUTAESAKU *et al.* 1972, TILNEY *et al.* 1973, BURTON *et al.* 1975, LA FOUNTAIN *et al.* 1977) and non-membranous components do not assume a dark-light-dark trilaminar appearance. Thus non-membranous microtubules retain their normal dimensions and appearance, save for enhancement of their protofilamentous substructure (Fig. 1). In other words membrane can be distinguished unambiguously from non-membrane.

Digestion of fixed tissue with driselase merely removes wall material, thereby making the plasmodesmata stand out more clearly. A relatively lucent sleeve of specialised wall material that surrounds each plasmodesma in conventional preparations (Fig. 10) is no longer seen, dense deposits appearing (Figs. 7–9 and 14–18), often in a helical configuration (*e.g.*, Fig. 8). The enzyme does not seem to influence structural preservation in the membranes or cytoplasm (see also WICK *et al.* 1981).

3.2. Longitudinal Image of Plasmodesmata

Plasmodesmata in *Azolla pinnata* roots are membrane-lined pores with more or less parallel sides and a length of 147 ± 32 nm (28). The lining is a continuation of the plasma membrane (Figs. 1–3 and 6–9). Desmotubules are seen as lucent rods lying in the longitudinal axis (Figs. 1–9). The clarity of the membranes after glut/p-form/tannic acid/$FeCl_3$ fixation is such that favourable longitudinal views show continuity of ER and desmotubule. The trilaminar structure of the ER is less and less apparent as it becomes tightly curved upon entering the plasmodesma. Nevertheless the lucent component of the desmotubule can be seen to be continuous with the lucent inner layers of ER membranes, both in stereo-pairs (Figs. 7–9), and also in some ordinary images (Figs. 2, 3, and 6). The lucent part of the desmotubule has a total diameter of 7.2 ± 0.8 nm (16). Some glancing sections show electron-lucent particles between it and the plasma membrane (Fig. 4); however these are not regularly seen, presumably because they are much smaller than the section thickness and are usually obscured by other superimposed material.

Section of embedded walls from macerated tissues show that many plasmodesmata survive, although they may be partially pulled out of the wall and damaged (Fig. 4). The desmotubule is retained even after such harsh processing procedures.

3.3. Transverse Images of Plasmodesmata

Fig. 19 *A* is a diagram of a plasmodesma, based on representative transverse sections of material fixed in glut/p-form/osmium tetroxide and glut/p-form/tannic

acid/$FeCl_3$, such as shown in Figs. 10–14. Transverse views of plasmodesmata consist of a series of concentric circles beginning with a central dense dot (radius AB in Fig. 19 *A*) surrounded by an electron-lucent circle (BC). The next circle is a mottled layer (CF) which upon image-reinforcement or in favourable micrographs (Figs. 11–14) is resolved into a set of relatively lucent spots in a denser matrix. These spots are not clearly imaged and are not always circular in profile, indeed it is by no means clear from the micrographs whether they are negatively-stained particles or gaps between positively-stained radial spokes. They have a "diameter", measured in the radial direction, of 4.5 ± 1.0 nm (37). In some cases reinforcement by Markham rotations at 40° increments suggested a total of 9 in the circle, but this is not claimed as a consistent feature (see Figs. 11–14). The final light (FG) and dark (GH) layers are part of the trilaminar plasma membrane. The electron-dense layer of the inner face of the plasma membrane is not demarcated from the dense matrix in which the "particles" lie. Dimensions of these components are given in Table 1 and in an idealised scale drawing (Fig. 19 *A*).

The dimensions of ER membranes, both single and appressed, in the cytoplasm of glut/p-form/tannic acid/$FeCl_3$ fixed material are presented in Fig. 19 *B* and Tab. 2 for comparison with those of plamodesmata. Major features are: (i) correspondence between the diameter of the central component of plasmodesmata (twice AB) and the combined thickness of two back-to-back outer leaflets (twice IJ), and (ii) correspondence between the thickness of the innermost electron-lucent layer of plasmodesmata (BC) and the electron-lucent component of an ER bilayer (JK).

Conventional glut/p-form/osmium tetroxide fixations

Table 1. *Dimensions of plasmodesmatal components as seen in transverse section*

Component (as in Fig. 19 *A*)	Glut/p-form/tannic acid/$FeCl_3$ (nm)	Glut/p-form/OsO_4 (nm)	Robards (1976) (nm)
AB	1.4 ± 0.3 (37)	1.8 ± 0.3 (25)	1.5
BC	2.2 ± 0.4 (37)	2.3 ± 0.4 (25)	2
CF	8.2 ± 0.9 (37)	9.0 ± 0.8 (25)	
FG	1.9 ± 0.7 (37)	1.6 ± 0.4 (25)	14
GH	3.6 ± 1.3 (37)	3.4 ± 0.8 (25)	
DE	4.5 ± 1.0 (37)	5.4 ± 1.8 (25)	
EF	1.7 ± 0.9 (37)	1.9 ± 0.6 (25)	

Table 2. *Dimensions of ER membranes in cells fixed in glut/p-form/tannic acid/$FeCl_3$*

Component (see Fig. 19 *B*)	Thickness (nm)	Component (see Fig. 19 *B*)	Thickness (nm)
IJ	1.5 ± 0.3 (8)	MN	3.9 ± 0.7 (40)
JK	2.2 ± 0.6 (16)	NO	2.1 ± 0.4 (40)
KL	3.0 ± 0.5 (16)	OP	4.0 ± 0.9 (40)

Fig. 1. The appearance of membranes and microtubules following preservation and staining in glut/p-form/tannic acid/$FeCl_3$. Plasma membrane (*P*), membranes of dictyosomes (*D*) and associated vesicles, tonoplast (*T*) and endoplasmic reticulum (*ER*) are all clearly trilaminar with a lucent central layer. Protofilaments can be seen in cross-sectioned microtubules (*e.g.*, arrowhead). A plasmodesma is preserved although the cell wall had been digested away by driselase treatment after fixation. × 140,000

Fig. 2. Continuity of endoplasmic reticulum (*ER*) and plasma membrane (*P*) through a plasmodesma. The lucent central portions of ER bilayers become the lucent portion of the desmotubule (between tips of small arrows), separated from the inner face of the plasma membrane by a mottled layer. Where the two membranes of the ER lie apposed to one another the thickness of the combined central dense layer is comparable to that of each dark layer of the separated membranes (areas such as in the squares in this Figure and in Fig. 1 are diagrammed in Fig. 19 and the dimensions of the components listed in Tab. 2). Glut/p-form/tannic acid/$FeCl_3$ – driselase digestion. × 175,000

Fig. 3. A preparation as in Fig. 2 but with the ER cisterna distended and approaching the neck of the plasmodesma parallel to the plasma membrane. × 175,000

Fig. 4. Glancing oblique section of a plasmodesma showing lucent particles (in a vertical row above the tip of the arrow) in the mottled layer between the inner face of the plasma membrane and the lucent portion of the desmotubule. × 175,000

Fig. 5. A fragment of a plasmodesma in a cell wall fraction obtained by centrifuging macerated root primordia. The plasma membrane bilayer and lucent portion of the desmotubule appear much as in normal preparations. The fraction was not digested with driselase and a sleeve of lucent material is visible surrounding the plasmodesma. × 175,000

Fig. 6. A group of plasmodesmata, probably all connected to the same cisterna of ER. Several show continuity between the lucent portion of the desmotubule and the lucent layer of the ER membranes (especially at arrowheads). Glut/p-form/tannic acid/$FeCl_3$ – driselase digestion. × 200,000

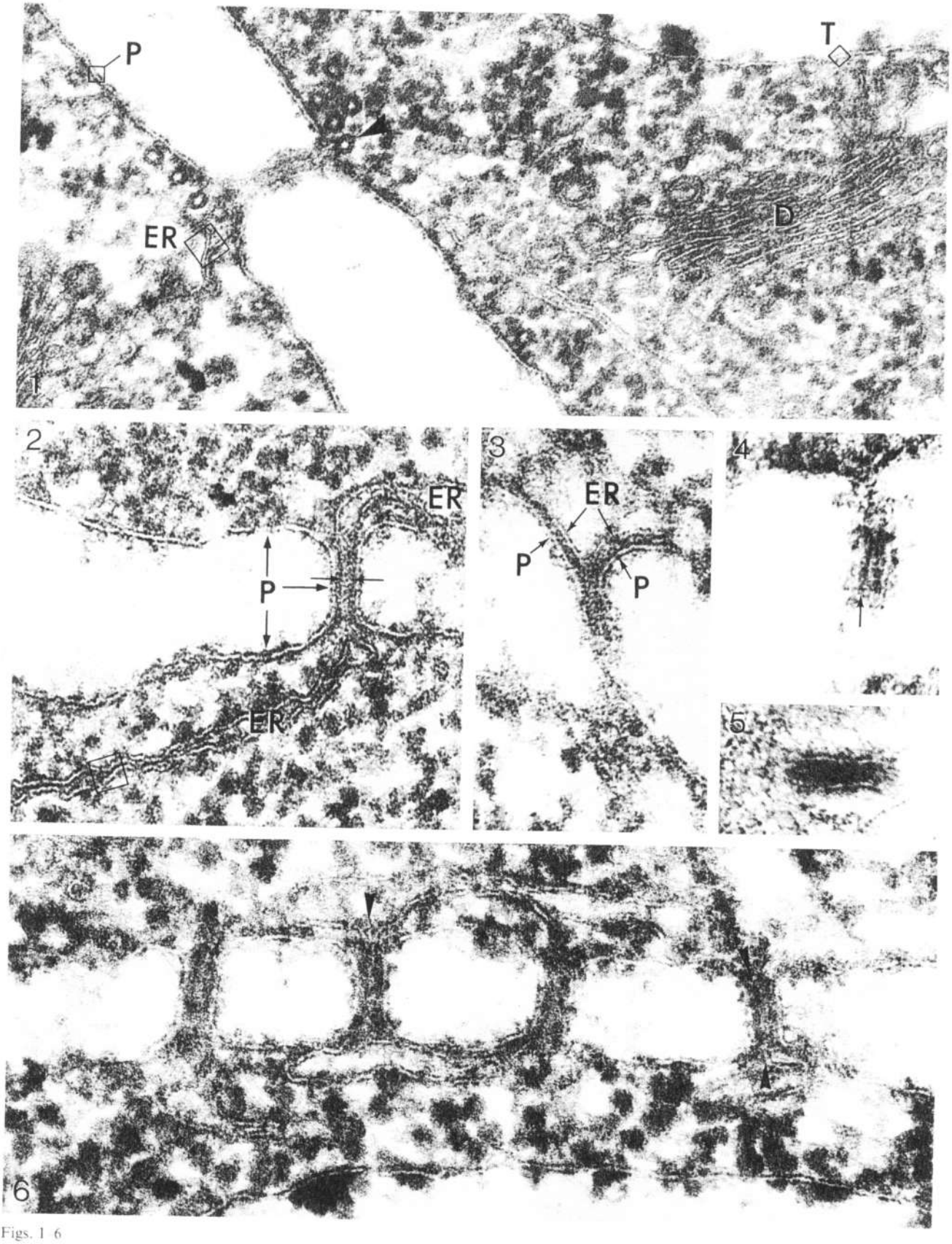

Figs. 1–6

differ from the above in that the layers are less clearly demarcated, especially in cytoplasmic membranes. However, conventional (Figs. 10 and 13) and tannic acid (Figs. 11, 12, 14, and 15) preparations are basically very similar, and also match images of plasmodesmata obtained by ROBARDS (1976) for another species of *Azolla* using a different tannic acid procedure. Both procedures indicate the presence of a ring of "particles".

3.4. Neck Region

The axial ER derivative and the inner face of the plasma membrane usually diverge at the neck region of plasmodesmata, leaving a cytoplasmic space between (Figs. 1, 2, 6, and 7–9). Transverse views showing more and more divergence are illustrated in Figs. 15–18. In Fig. 15 the central dot (AB), the surrounding electron-lucent ring (BC), and the ring of "particles" appear much as they do in the middle of the plasmodesmatal canal but the plasma membrane is less distinct, no longer being normal to the plane of section. In Figs. 16–18, the central density (AB) and surrounding electron-lucent ring (BC) are progressively replaced by what is more clearly a trilaminar membrane, with a distinct lumen rather than a central dot. Such views presumably correspond to the zone where the ER tapers towards the desmotubule (Figs. 1–3 and 6–9). The mottled zone (CF) also increases in width (Figs. 17 and 18).

Sometimes the same ER cisterna may be seen to be associated with adjacent plasmodesmata (Fig. 6). Extensions of the ER that approach the plasmodesmata usually do so approximately normal to the cisterna (Figs. 1, 2, and 6). Alternatively, a distended cisterna may closely follow the contour of the plasma membrane around the neck of the plasmodesma (Fig. 3). A coating of particulate material on the outer electron-dense leaflet of the ER near the orifices appears to continue on down into the plasmodesma in such cases (Fig. 3).

4. Discussion

4.1. Effect of Tannic Acid

Tannic acid precipitates proteins (FUTAESAKU *et al.* 1972) and during fixation shields of tannic acid-heavy metal complexes are thought to be formed around protein macromolecules and subunit particles, conferring negative contrast on such structures (TILNEY *et al.* 1973, LA FOUNTAIN *et al.* 1977, OLESEN 1978, 1979, PIERSON *et al.* 1979, SEAGULL and HEATH 1979, JUNIPER and LAWTON 1979). The lucent spots in the mottled layer (CF in Fig. 19 *A*) will therefore be referred to as particles in what follows, although reservations about their structure remain.

The negative contrast of the ring of particles in the plasmodesmata of *A. pinnata* roots after tannic acid fixation is similar to that seen by OLESEN (1979) in the plasmodesmata of *Epilobium hirsutum* L. roots (a tissue high in natural tannins) and *Salsola kali* L. leaves and by ROBARDS (1976) in plasmodesmata of roots of *Hordeum vulgare* L. and *Azolla filiculoides* after similar treatment. The ring of particles can also be seen in conventionally-fixed *Azolla* plasmodesmata, probably because this tissue too contains natural tannins which are released during fixation (GUNNING and STEER 1975). This image of the ring of particles is reminiscent of that of protofilaments in microtubules after tannic acid fixation (Fig. 1), although the number of units is smaller (TILNEY *et al.* 1973, PIERSON *et al.* 1979).

Some of the structure seen in material fixed in tannic acid may be present because the tannic acid-heavy metal complex stabilizes them against shrinkage or extraction that would otherwise occur during dehydration and subsequent processing (SIMONESCU and

---

Figs. 7–9. Stereo pairs of plasmodesmata, fixed in glut/p-form/tannic acid/$FeCl_3$ and digested with driselase; all tilt angles 15°. × 150,000

Fig. 7. The central part of the plasmodesma is covered by plasma membrane within the thickness of the section so that details of the desmotubule are partially obscured. Indications of ER-desmotubule continuity are seen at the orifices

Fig. 8. The upper portion of this plasmodesma is covered by plasma membrane. The mottled layer between the ER and the plasma membrane extends for some distance (between arrows) around the neck region. ER-desmotubule continuity is again seen at the lower orifice. The arrowhead indicates a putative connection between the ER and the plasma membrane near the orifice of the plasmodesma

Fig. 9. This plasmodesma dips downwards until it is just being grazed by the lower surface of the section, then it turns upwards towards the observer at right angles to the plane of section. ER-desmotubule continuity (lucent portions) is seen at the upper left orifice; in the cross-sectioned view, the "central rod", the inner electron-lucent annulus, the mottled particulate layer and the plasma membrane bilayer (dark-light-dark) are all visible, especially at the left hand side of the profile. Face-to-face membranes are seen at lower right (arrow); as in Figs. 1 and 2, the dark layers merge to become less than twice as thick as any single dark surface layer

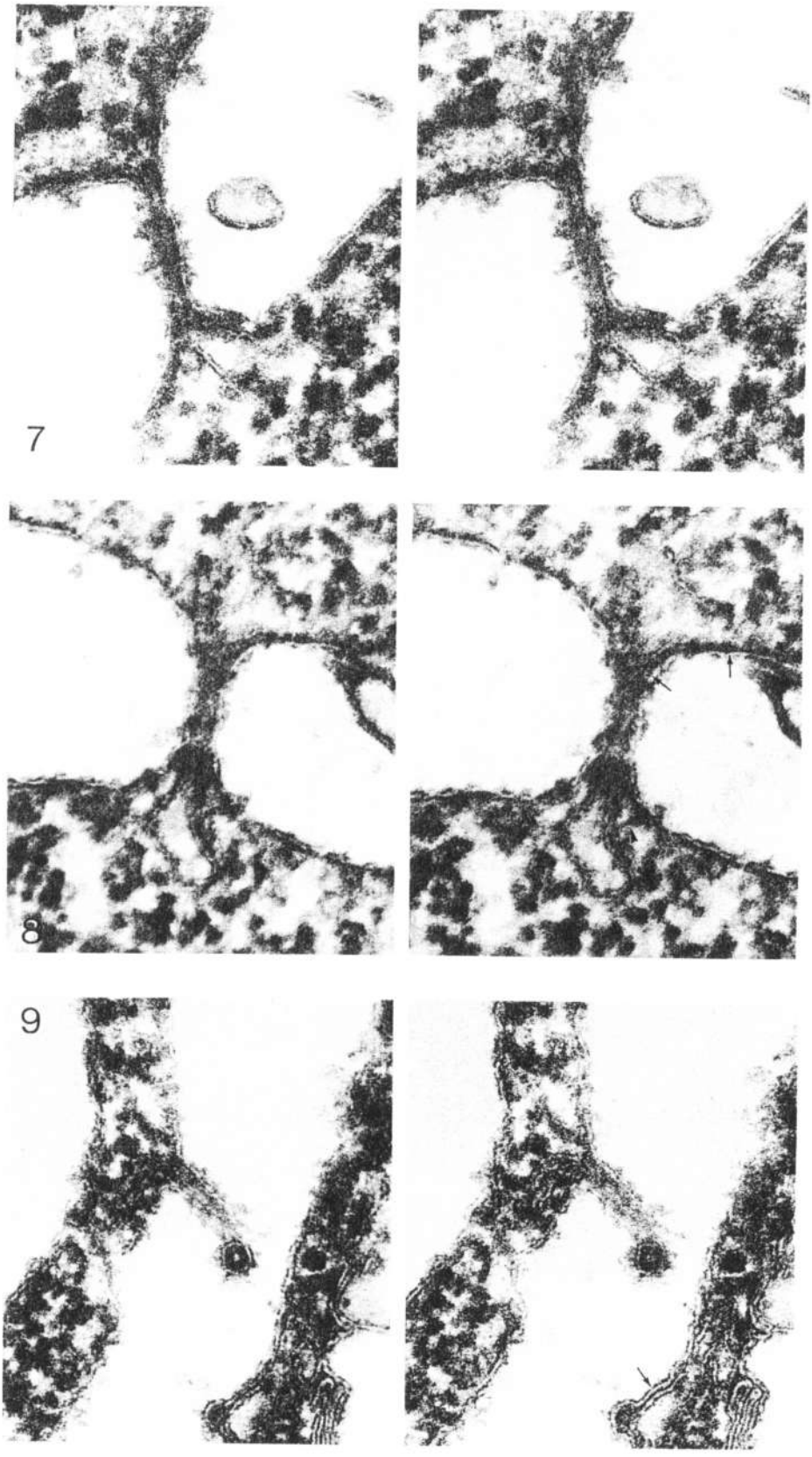

Figs. 7–9

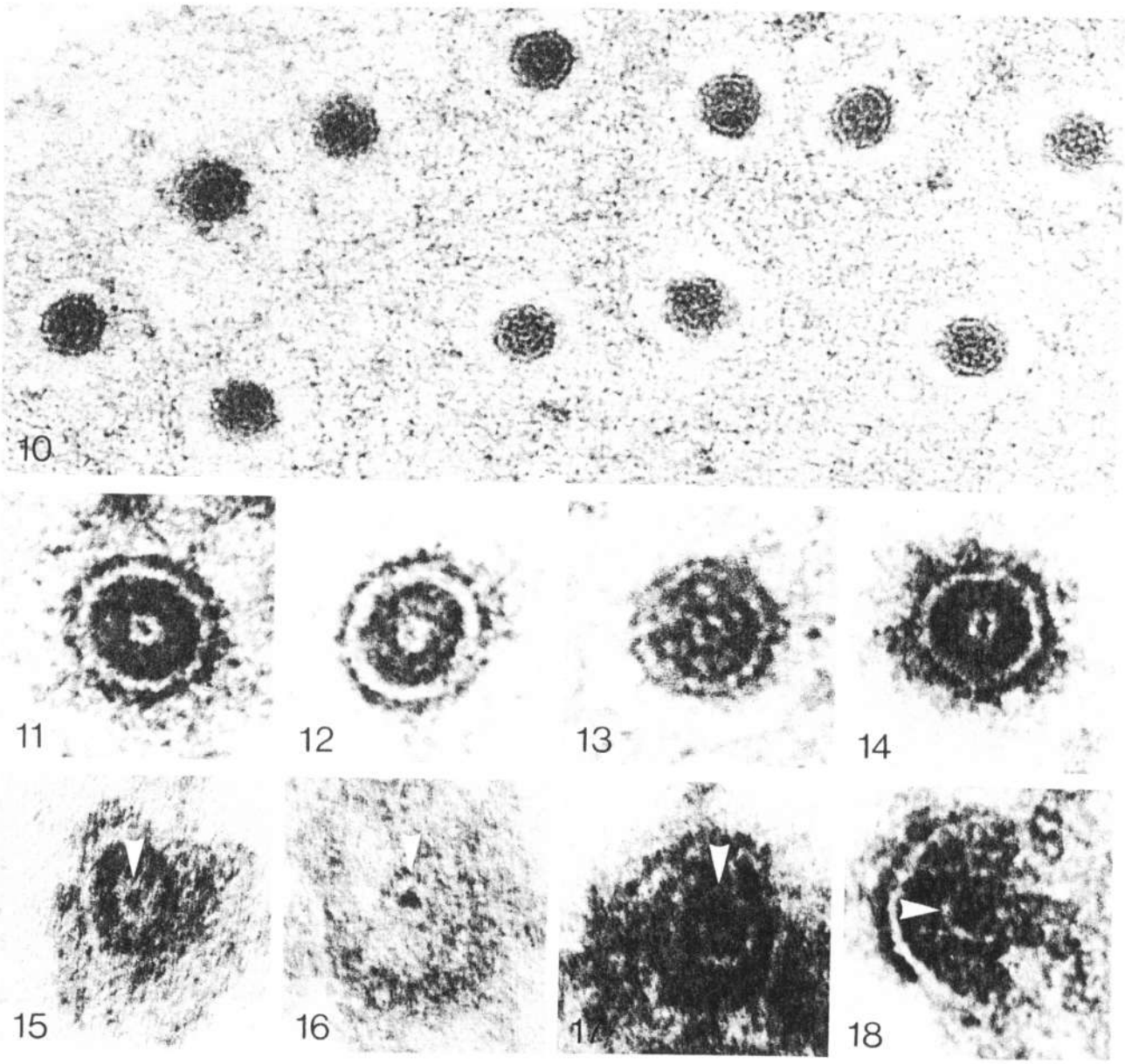

Figs. 10–18. Transverse sections of plasmodesmata

Fig. 10. Glut/p-form/osmium tetroxide fixation with no digestion. Lucent wall sleeves are visible. × 280,000

Figs. 11–14. Views of selected plasmodesmata. Fig. 13 shows conventionally-fixed material whereas the others were fixed in glut/p-form/tannic acid/$FeCl_3$; Fig. 14 is the only one illustrating material that had been digested with driselase. All show the same set of annuli – central dense rod, lucent ring, dense mottled layer, and plasma membrane bilayer. Details within the mottled layer are not resolved. All × 640,000

Figs. 15–18. Transverse sections through neck regions. The inner electron-lucent annulus is marked by arrowheads. Fig. 15 – central dense rod surrounded by a lucent annulus and mottled layer, much as in Figs. 11–14; Figs. 16–18 – expansion of the central density, but still surrounded by a lucent annulus. The visibility of the plasma membrane bilayer varies, presumably according to its orientation with respect to the plane of section. The thickness of the mottled layer also increases in a variable fashion according to the shape of the plasma membrane at the neck of the plasmodesma relative to that of the lucent annulus. × 640,000

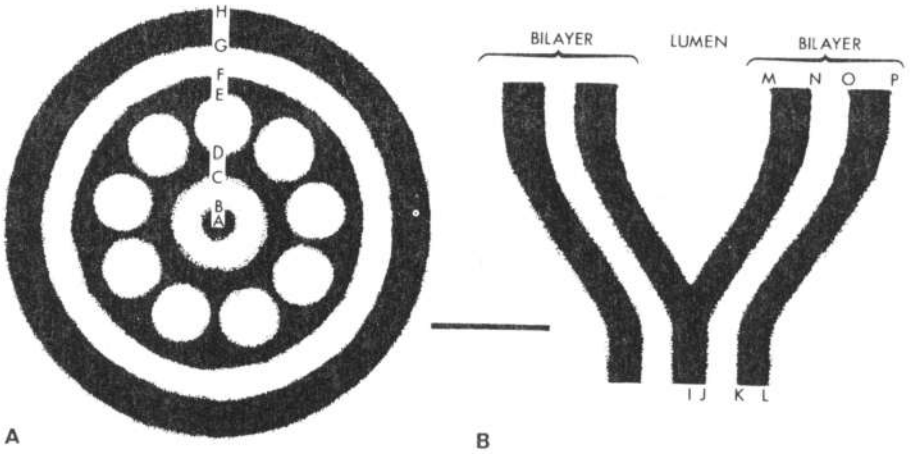

Fig. 19. Idealised diagrams drawn approximately to scale illustrating: (*A*) components seen in transverse sections of plasmodesmata (as Figs. 10–14); dimensions of successive lettered annuli are given in Tab. 1; (*B*) ER bilayers meeting face to face; dimensions of lettered layers are given in Tab. 2. Scale marker 10 nm

SIMONESCU 1976, OLESEN 1978). Bearing these features in mind, the ultrastructure of plasmodesmata, and especially the desmotubule, can now be considered.

4.2. Structure of the Desmotubule

Several models for the structure of the desmotubule have been put forward (LÓPEZ-SÁEZ *et al.* 1966, ROBARDS 1968, 1971, SEMENOVA and TAGEEVA 1972, BRIGHIGNA 1974) but they are still equivocal, the structures involved being close to the limit of resolution of available techniques (reviewed by ROBARDS 1976).

The model of ROBARDS (1971) depicts the desmotubule as a modified membrane (composed largely of protein subunits) in direct continuity with the ER, with an open lumen and an axial "central rod" of unknown nature (possibly artefactual). On the basis of Markham rotations it has been suggested that the number of subunits seen in transverse sections of the wall of the desmotubule is 11 (ROBARDS 1968), 14 (ZEE 1969) or 9 (OLESEN 1979).

Interpreting the plasmodesmata of the *Azolla pinnata* root on this model, the ring of electron-lucent particles, along with surrounding electron-dense material (CF), might constitute the desmotubule wall, while the inner lucent ring (BC) would be the desmotubule lumen. However, this model is inconsistent with (a) dilation of the central rod into a lumen at the neck region (Figs. 15–18), and (b) continuity of the lucent inner layer of the ER with the inner lucent ring (BC) of the plasmodesmata, as distinct from continuity of the particle zone with ER membrane—which is *not* observed. The present results suggest that the inner electron-lucent ring (BC) is a negatively-stained inner layer of a membrane, continuous with its counterpart in the ER.

A second, less popular, model, but one which has not been disproved, is that of LÓPEZ-SÁEZ *et al.* (1966), with subsequent variations by SEMENOVA and TAGEEVA (1972) and BRIGHIGNA (1974). Fig. 20 shows a version of this model, modified to take into account the ring of electron-lucent particles seen in *Azolla* and indeed in many other plasmodesmata. The essential feature is that the central rod represents tightly curved and packed inner electron-dense leaflets of extensions of ER membranes (AB), while the inner electron-lucent ring seen in plasmodesmata (BC) is continuous with the central, lucent layer of the ER membrane. There is no lumen in the desmotubule in this model. The electron-dense area immediately outside this electron-lucent ring (CD) would then be the outer, or cytoplasmic, leaflet of the ER membrane, which is not clearly demarcated from the density in which the particles lie. The electron-lucent particles may represent the particles sometimes observed on the outside layer of ER near plasmodesmata. At any event they are between the inner (cytoplasmic) face the plasma membrane and the outer (also cytoplasmic) faces of the ER.

In areas where the two membranes of an ER cisterna are in close contact with one another, such as in Fig. 2, the inner electron-dense leaflets appear to merge. Their combined thickness (twice IJ) is comparable to the normal width of the inner electron-dense layer of a single ER membrane (MN) (Tab. 2). A similar phenomenon is seen when other membranes lie in contact (Fig. 9). Although the ER membranes seen appressed to each other in the cytoplasm are not in a tubule, as

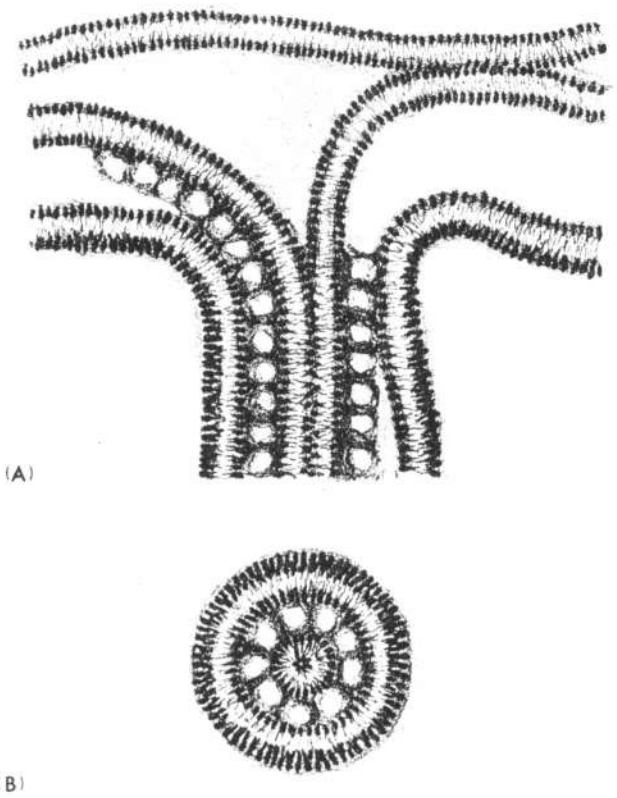

Fig. 20. Diagram illustrating the proposed relationship between ER and plasma membrane bilayers and plasmodesmatal components, shown in longitudinal (*A*) and transverse (*B*) views. Apposed ER membranes are shown at upper right; (*B*) shows the situation throughout plasmodesmata of *Azolla* root primordia, envisaged to apply also to neck constrictions in other situations: as shown at lower right in (*A*) the cytoplasmic annulus may become distended within the cell wall (though not illustrated here, so may the desmotubule)

proposed for the desmotubule, the merging of the apposed leaflets gives some indication of the size and type of staining effect that could be expected on the axis of a tubule that is so tightly curved that there is essentially no lumen. It can be seen from Tab. 2 that the diameter of the combined appressed electron-dense leaflets accords well with that of the central rod (twice AB), as does the width of the central lucent layer of the ER membrane (JK) with that of the inner electron-lucent ring in the plasmodesmata (BC).

The above dimensions and comparisons suggest that the version of the LÓPEZ-SÁEZ *et al.* model shown in Fig. 20 is feasible. This interpretation of plasmodesmatal structure is also supported by evidence obtained by impregnating the lumen of the ER with osmium or zinc-osmium or by staining it with ferrocyanide (HAWES *et al.* 1981, HEPLER 1982 and references therein). Such procedures show that in mature plasmodesmata the ER lumen becomes severely attenuated, or even abolished, at the desmotubule. For example, Fig. 22 of HAWES *et al.* (1981) shows only a very fine strand of zinc-osmium stain passing along the axis of the plasmodesma (presumably in the desmotubule). It is 1–2 nm in diameter and thus corresponds with the dimensions of the central rod, as compared with the total diameter of the desmotubule, cited as 9.6 nm, slightly larger than that described here. However, other micrographs obtained by HAWES *et al.* show a wider axial stained strand (Dr. B. JUNIPER, personal communication), and it is not known whether the zinc-osmium procedure can stain part of the membrane, as well as the lumen, of the ER. Also, rapidly-frozen samples processed by freeze-substitution retain desmotubules that closely resemble conventionally-fixed ones (OVERALL, unpublished), and negatively-stained cryo-sections of rapidly-frozen fixed or unfixed specimens show electron-lucent desmotubules, probably corresponding to AC in Fig. 19, of diameter 5–7 nm (VIAN and ROUGIER 1974). It therefore seems improbable that the high curvature of the ER bilayer in the desmotubule results from shrinkage during specimen preparation.

4.3. Molecular Packing in the Desmotubule

ROBARDS (1968, 1971), following the then prevailing views of J. D. ROBERTSON on unit membranes, argued that the LÓPEZ-SÁEZ *et al.* (1966) model of the desmotubule was in error because a bilayer membrane could not become curved into the necessary tight radius. A corollary was that the desmotubule, if it is a modified membrane, must have a lower curvature, *i.e.* must have an open lumen: it then followed naturally to equate the electron-lucent core of the desmotubule with that open lumen and to dismiss the central rod, despite its presence in the majority of cases, as an unknown structure or an artefact. A return to the LÓPEZ-SÁEZ *et al.* model, as advocated here, demands a detailed examination of molecular packing in the proposed structure. The following analysis shows, with some provisos, that it is possible for molecules whose average geometry is similar to that of the constituents of the ER to form a cylindrical bilayer with the dimensions suggested by electron micrographs of desmotubules.

First, it is not self-evident how molecular geometries *in vivo* may be deduced from a stain in an electron micrograph. It is here assumed that the electron-lucent annuli have precisely the dimensions of the non-polar regions of a fluid mosaic membrane, and that

all head groups of the lipids in the desmotubule (and the highly polar regions of intrinsic proteins, if present) lie either within a cylinder of radius 1.4 nm (AB) or without a cylinder of radius 3.6 nm (AC). With respect to the desmotubule, the assumption is supported by the observed continuity of BC with the electron-lucent inner layer of the ER. Similar continuity of an electron-lucent annulus (FG) with a lucent inner layer of a membrane is seen much more obviously in the case of the plasma membrane. Calculations of geometry depend very strongly on the value of the inner radius, however, and if the stain defined a line that is further from the hydrocarbon chains than the carboxyls that delimit the head groups, the molecular packing would be rather less dense than calculated below.

Second, the ER comprises lipids, about whose composition and geometry there is information from several sources, and proteins whose exact nature and shape are in general unknown. The ER of castor bean endosperm contains about 60% lipids by weight (DONALDSON and BEEVERS 1977). Lipids have a polar head group which, in membranes, is immersed in the water adjacent to the membrane, and hydrocarbon tails which, due to hydrophobic interaction, contact either each other or the non-polar regions of intrinsic proteins (TANFORD 1973). For usual biological temperatures, these tails are fluid and capable of packing around intrinsic proteins, considered to be more rigid than lipid in the fluid mosaic model (SINGER and NICHOLSON 1972). In the present context packing of proteins is less important than that of lipids. Since proteins, though large, are present only in very small molar concentrations, the entropy of demixing for proteins is not large, and such proteins as are not easily packed into the desmotubule may be present only in negligible concentrations. Further, since the thickness proposed for the hydrophobic region of the desmotubule is the same as that of the planar ER, some proteins which span the ER may fit easily into the desmotubule, particularly any "conically" shaped proteins, as envisioned by ISRAELACHVILI (1978).

There is a conceptually simple theory which has quantitative success in explaining the equilibrium shapes and sizes of aggregates of lipids in terms of their molecular geometries (ISRAELACHVILI *et al.* 1977, MITCHELL and NINHAM 1981). The theory postulates that: (i) lipid tails are highly incompressible and so a tail volume v may be ascribed to any lipid such that any aggregate which has a low free energy must provide this volume for each tail (or pair of tails); (ii) the hydrocarbon tail-water interface has a very large surface tension, and is opposed in large lipid aggregates by an equally strong repulsion between head groups. The area per head group in any aggregate with low free energy must be very close to the value of that area, a_o, at which these forces are equal; (iii) at physiological temperatures, lipid tails behave as an essentially incompressible hydrocarbon fluid, occupying almost any shape with volume v, provided they are not extended beyond a length, l_c, which may also be ascribed to each lipid. A thermodynamic analysis shows that tail packing constraints determine the geometry of lipid aggregates (ISRAELACHVILI *et al.* 1977). For any lipid, the most stable aggregate is approximately the smallest possible arrangement which packs the lipids at their prescribed values of v and a_o and where no tails are extended beyond l_c.

The above theory is primarily concerned with micelles and vesicles and cannot be applied to biological systems without caution, since it refers to thermodynamic equilibrium and living systems are not at equilibrium, their membranes being unstable with respect to small vesicles. In the case of the desmotubule it is not clear what mechanical forces might influence the free energy of its molecules, *e.g.* by compression from the surrounding structures or tension between the terminal ER connections. However, it is extremely unlikely that intra-cellular variations in pressure and tension are large enough to significantly alter a_o and v. To change v by say 5% would require a change of pressure of 50 MPa, assuming that the hydrocarbon chains have the same compressibility as bulk hydrocarbon. To change a_o by 5% would require a change in membrane tension of $12\,mN \cdot m^{-1}$, assuming that the area elastic modulus of the membrane is similar to that of the plasma membrane, whereas a tension of $4\,mN \cdot m^{-1}$ ruptures the plasma membrane of plant protoplasts (WOLFE and STEPONKUS 1981). In fact, if the free energy of molecules in the desmotubule were very much higher than that of similar molecules in the ER, the desmotubule would tend to coalesce with the ER. Hence any differences in free energy between the two structures are probably not many times kT per molecule (where k is BOLTZMANN's constant and T the temperature). While such differences may have concequences for the molecular composition of the desmotubule *vis-à-vis* the ER (a point to be examined later), it may be concluded that similar tail packing constraints should apply to similar molecules in the ER and the desmotubule, and further, that if the compositions of the ER and of the desmotubule are the same, then both structures will have the same average value of a_o and v/a_o. In the first stage of

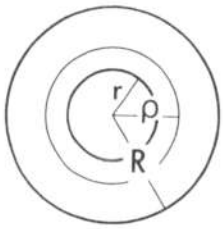

Fig. 21. Radii used in calculating dimensions available for lipid head groups in the central rod (r corresponding to AB in Fig. 19 *A*), for associated hydrocarbon tails ($\rho - r$), and for hydrocarbon tails of the outer half of the cylindrical bilayer ($R - \rho$). ($R - r$ corresponds to BC in Fig. 19 *A*)

the following analysis an average value of a_o and v/a_o appropriate to lipid is ascribed to each structure, which is then treated as if it contained only that one average component. It emerges that both structures satisfy the same packing criteria, and thus could be composed of the same molecules without incurring large energies of deformation.

The equilibrium version of the molecular packing theory (ISRAELACHVILI *et al.* 1977) shows that cylindrical vesicles are unstable with respect to spherical vesicles because of end effects: the aggregation number of a cylindrical vesicle must be larger because of the spherical ends. This constraint does not affect the present problem (where the aggregation number is effectively infinite) so entropies of aggregation can be neglected and packing criteria used to examine whether a cylindrical bilayer is energetically possible.

Consider a cylindrical portion of length l whose section is shown in Fig. 21. ρ is the radius of the average dividing surface between the inner and outer leaflets. The interfacial area and tail volume available for the outer leaflet tails are

$$A_o = 2\pi R\, l \text{ and } V_o = \pi(R^2 - \rho^2)l$$

and for the inner leaflet tails

$$A_i = 2\pi r\, l \text{ and } V_i = \pi(\rho^2 - r^2)\, l$$

For an average lipid molecule:

$$\frac{v}{a_o} = \frac{R^2 - \rho^2}{2R} = \frac{\rho^2 - r^2}{2r}$$

whence $\rho^2 = Rr$. With $r = AB = 1.4\,nm$ and $R = AC = 3.6\,nm$, this yields $\rho = 2.2\,nm$ and $v/a_o = 1.1\,nm$ for molecules in the desmotubule. The value of v/a_o for the molecules forming the planar regions of the ER is simply half the thickness of the electron-lucent regions of the membrane, thus the electron micrographs show that $v/a_o = 1.1\,nm$ for those regions also. The other packing constraints are that there are both maximum and minimum values for the average chain length. Thus the maximum, l_c, must be $\geq$ the average available length, which is $R - \rho = 1.4\,nm$ in the outer leaflet of the desmotubule. CHRISPEELS (1980) reports that, of the phospholipids which comprise 82% of the lipids of the ER of castor bean endosperm, the tail composition is: palmitic (40%), linoleic (36%), oleic (12%), stearic (8%) and linolenic (4%). For acyl chains of these lengths, l_c is considerably larger than 1.4 nm (ISRAELACHVILI *et al.* 1977), so this constraint is satisfied. The minimum length into which chains can be packed, which depends on the nature of the lipid, is less clearly defined but is estimated to be within the range $0.2\,l_c - 0.5\,l_c$ (MITCHELL and NINHAM 1981). For the inner leaflet of the desmotubule the available space is $\rho - r = 0.8\,nm$. This is 0.42 of l_c in egg lecithin, and since tails of ER lipids probably have similar lengths, packing is not excluded.

From the excellent agreement in v/a_o, and the satisfying of $0.2\,l_c - 0.5\,l_c \leq$ chain length $\leq l_c$ for both leaflets, this analysis shows that fluid molecules with the average geometry of those in the ER can form the proposed desmotubule without violating the packing criteria of the hydrocarbon regions. Packing of the head groups can now be considered.

One of the simplifying assumptions of the lipid packing theory of ISRAELACHVILI *et al.* is that all the steric properties of the head group may be incorporated in the single parameter, a_o. Provided that the curvature of the lipid-water interface is sufficiently low that it may be locally treated as planar, those lipids with an area density of $1/a_o$ should interact identically whatever the gross configuration of the aggregate, and so this postulate is justified. In the lipid packing theory, the minimum size of vesicles is determined by the extent to which chains may be straightened in the outer leaflet, subject to all other geometric constraints; and it is assumed that there is sufficient volume inside the vesicle for the head groups of the inner leaflet to pack without incurring a steric repulsion substantially greater than that among head groups at a planar interface. The head group-hydrocarbon interface of the inner half of the bilayer proposed here has a rather higher curvature ($1/r + 1/\infty = 0.71\,nm^{-1}$) than that of the smallest

vesicles considered by ISRAELACHVILI *et al.** (*e.g.*, for a spherical vesicle of egg phosphatidylcholine, the corresponding inner curvature is about 0.3 nm^{-1}). Thus, while the quantitative success of the packing theory for predicting vesicle sizes suggests the legitimacy of the local planar approximation for curvatures less than about 0.3 nm^{-1}, there is no guarantee that this approximation, and the corollary that head group interactions are all included in a_0, hold for the much tighter packing inside the proposed cylindrical desmotubule.

Cylindrical vesicles are unstable with respect to spherical vesicles, hence there are no reports of vesicles with highly curved inner surfaces with which to compare the head group packing in the proposed desmotubule. The energy requirement for packing lipid head groups at this curvature therefore cannot be assessed. However, it *can* be shown that at the optimal area density $1/a_0$, there is enough room inside this cylinder for lipid head groups and their hydration shells.

The thickness of the lucent region of the ER gives a value of v/a_0, but v and a_0 may not be determined from the micrographs. v may be estimated from the molar volumes of hydrocarbons determined by REISS-HUSSON and LUZZATI (1964): $V_{CH} = 0.0205\,nm^3$, $V_{CH_2} = 0.0270\,nm^3$ and $V_{CH_3} = 0.0540\,nm^3$ at 25 °C. Using the acyl frequencies given above, the weighted average volume of a pair of phospholipid tails is calculated to be 0.904 nm^3. Using $v/a_0 = 1.1$ (see above), this gives an average a_0 of 0.82 nm^2.

The number of head groups per unit length of the inner surface of the hydrocarbon annulus is $n = 2\pi r/a_0$, and from this value of a_0, $n = 10.7\,nm^{-1}$. The volume per unit length within the annulus is πr^2, and so the available volume per head group is $a_0\, r/2 = 0.57\,nm^3$. The volume of the head group (including carboxyl groups) of phosphatidylcholine is calculated from the molar volume of egg lecithin by TARDIEU *et al.* (1973), who obtained the value of 0.36 nm^3, *i.e.*, 63% of the *available* volume in the central rod. Data from which to calculate the head group volume for the other lipid components are not available. The major lipid components listed for the ER of castor bean endosperm (DONALDSON and BEEVERS 1977) are phosphatidylcholine (PC), (40.4% of phospholipids), phosphatidylethanolamine (PE), (32.6%) and phosphatidylinositol (PI), (16.6%). Compared to PC (whose head group has a molecular wt, $mw_H = 301$), PE has a smaller head group ($mw_H = 269$) in which three hydrogen atoms replace three methyl groups of PC. The head group of PI has a higher molecular weight (409). Apart from phospholipids (82% of total lipids), the only other substantial lipid components are free fatty acids (14% of total lipids) and diacyl and triacyl glycerol (3%). These components have small head group volumes per chain. From the foregoing data, the average head group volume of ER lipids is probably not more than that of PC, *i.e.*, 0.36 nm^3. Thus in general it is reasonable to conclude that the head groups, without hydration shells, occupy not more than 63% of the volume within the central rod of the desmotubule (radius AB in Fig. 19 *A*). Put another way, there is room within the central rod for at least 7.1 water molecules per lipid head group*. Since head group volume is calculated from hydrated bilayer density, any effect on the local density of water is implicitly included.

The head groups are obviously not fluids that may be squeezed into an arbitrary shape with sufficient volume. Explicit calculations about the packing of these groups cannot be made but we can show with molecular models that, at the required packing, there is sufficient space in the given shape to pack the head groups without steric hindrance. Ascribe to PC, the most common lipid, with a typical head volume, the average area per lipid of 0.82 nm^2 and for simplicity depict this

---

* If vesicles with large inner surface curvatures are prohibited by packing constraints, why is the structure proposed here not similarly prohibited? The answer is in the difference between cylindrical and spherical geometries. Simple geometric calculations show that, for the same v/a_0, spherical bilayers must be thicker than cylindrical bilayers. A spherical vesicle with the same inner curvature as our proposed cylinder (*i.e.* with inner radius $r_s = 2.8$ nm) will have an outer radius R_s satisfying

$$\frac{R_s^3}{3}\left(\frac{a_0}{v}\right) - R_s^2 - r_s^2\left(1 + \frac{r_s}{3}\left(\frac{a_0}{v}\right)\right) = 0$$

(where r_s and R_s refer to inner and outer head group-hydrocarbon layer interfaces respectively).

For the phosphatidylcholine vesicles considered by ISRAELACHVILI *et al.*, $a_0/v = 0.66\,nm^{-1}$ and so $R_s = 6.1$ nm. The *outer* tails would, on average, have a radial length of 2.2 nm, in excess of the value of l_c for lecithin (1.9 nm).

* The value of v/a_0 used above is rather smaller than that given by ISRAELACHVILI *et al.* for egg lecithin (1.5 nm), and will lead to a value of a_0 larger than that estimated for egg lecithin from collapsed monolayer densities (0.72 nm^2). We do not know whether this difference arises from a real difference in v/a_0 between the two systems (due either to their different compositions, or their different bathing media) or from a different definition or measurement of the thickness of the hydrocarbon regions. Use of ISRAELACHVILI's value of a_0 for egg lecithin gives a value of 4.4 water molecules per head group in the desmotubule. However the ER is thinner than egg lecithin bilayers and so the low value of a_0 is probably not relevant here.

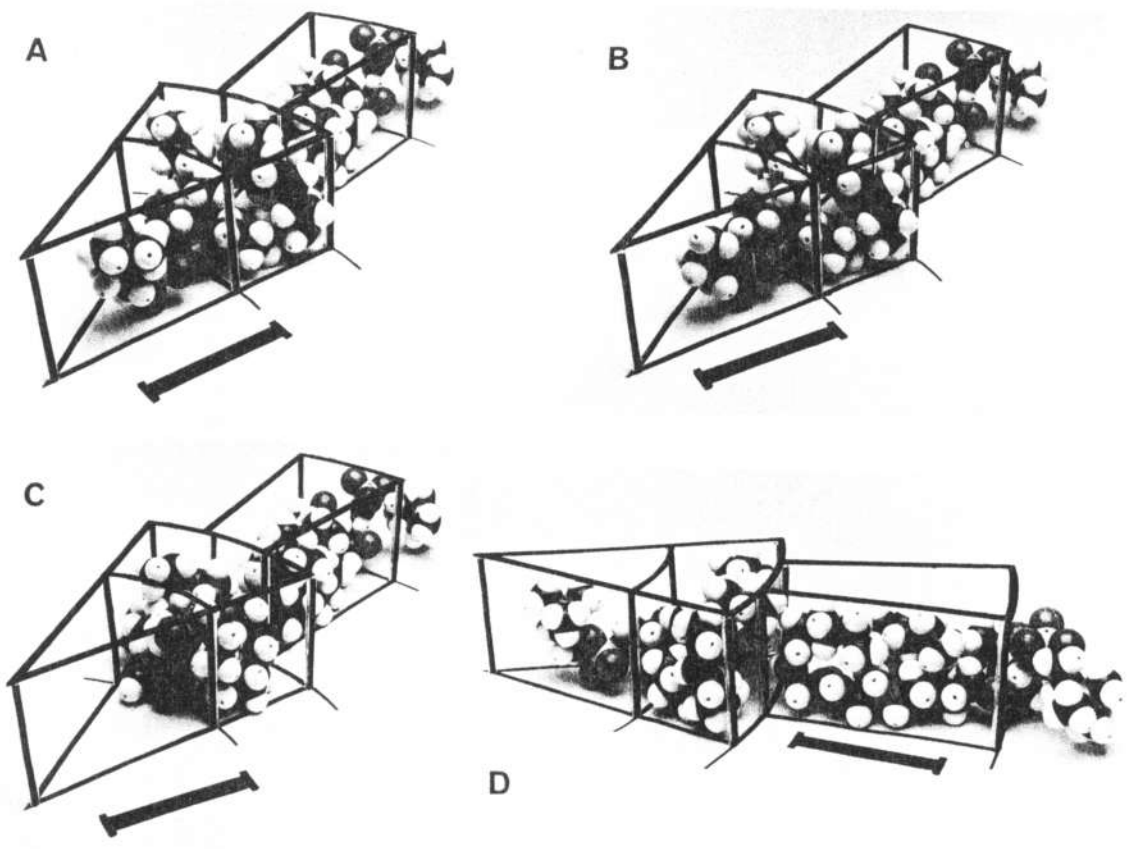

Fig. 22 *A*, *B*, *C*, *D*. These photographs show a scale model of the proposed molecular packing, with the scale bar representing 1 nm. The three concentric arcs have radii r, ρ and R (Fig. 21), and two cylindrical sectors have been constructed with the average lipid area a_o at the inner and outer hydrocarbon-water interfaces. In (*A*) and (*D*), molecules of palmitoyllinoleylphosphatidylcholine are shown. (PC is the most common lipid and has a typical head group volume; the two most common hydrocarbon chains are palmitic and linoleic, though it is unknown which chains are attached to which head groups). The PC head group fits easily into the inner sector. Note that the tail packing represented is an average only; no single tail would be expected to pack as shown (see GRUEN 1980 for a detailed discussion). (*B*) shows the same arrangement except that the next most common lipid head group, that of phosphatidylethanolamine, replaces that of PC at the inner interface. (*C*) shows how two free fatty acid molecules (again palmitic and linoleic) would pack in the same area. Though free fatty acids comprise only 12% of all ER lipids, one might expect them to be overrepresented in the inner leaflet of the desmotubule if head group packing were a limiting condition. Molecular models of this type are not constructed simply to one scale because of the geometric complexity involved. The scale shown here accurately represents the C–C bond, so that the overall dimensions of the molecule and the positions of the atomic centres are reproduced to scale. Using this relation, however, the radii of individual atoms is less than their van der Waals radii; in the case of hydrogen, by about 20%. Thus a complete scale model of the tails, say, would have the same length as those shown, but would be rather thicker

area as a portion on the cylinder bounded by two straight vertical sides and two horizontal arcs, all of length $\sqrt{0.82\,\text{nm}^2} = 0.91\,\text{nm}$. This geometry is shown in Fig. 22, which gives visual confirmation that the packing criteria for both head groups and hydrocarbon tails are satisfied by the proposed model of the desmotubule.

Packing calculations become much more complicated for two components than for one (CARNIE *et al.* 1979), and forbidding for realistic models of biological membranes, however some qualitative remarks may be made. First, molecules are free to diffuse laterally in the SINGER-NICHOLSON model of the membrane and entropy would be maximised if lateral diffusion continued until the compositions of the desmotubule and the ER with which it is continous were the same. This tendency might be overcome to some extend by external forces which lower the free energies of different species of molecules by differing amounts in one region. Second, small differences in packing energies between different molecules in the same region of a membrane could also overcome to some extent the mixing entropy. Thus molecules with larger v/a_o or larger l_c preferentially associate in thick regions and/or convex surfaces of the

membrane, and conversely (Israelachvili 1978). In the desmotubule for example, there might well be a higher proportion of PE and free fatty acids in the inner monolayer of the cylinder than in the outer (though for these lipids the effect would be mitigated by electrostatic repulsion to some extent).

To produce an *e*-fold change in the concentration of one species the local free energy per molecule must be lowered by the order of kT. Such a change for molecules of the size of lipids can be expected from a change in membrane tension of 5–10 $mN \cdot m^{-1}$ or other forces with this magnitude. These are large compared with tensions found in relatively flat, macroscopic membranes, or membranes in equilibrium (Gruen and Wolfe 1982), indeed, as already noted, the plant plasma membrane ruptures under a tension of about 4 $mN \cdot m^{-1}$ (Wolfe and Steponkus 1981). On the other hand these tensions are small compared to the principal tension stabilising the membrane (the surface energy of a water-hydrocarbon interface is typically 50 $mN \cdot m^{-1}$) and since the desmotubule is neither flat nor macroscopic it could possibly be subject to tensions as large as several $mN \cdot m^{-1}$. It is thus possible that the composition of the desmotubule is substantially different from that of the ER as a whole, with concentrations of some lipids varying by as much as several-fold, and concentrations of proteins which are larger and therefore have a distribution more sensitive to external forces (Gruen and Wolfe 1982) ranging more markedly.

This possibility does not alter the conclusion that the desmotubule can be a tightly curved cylindrical bilayer. Since a bilayer with the *same* composition as the ER is not prohibited by geometry from forming a cylinder of the given dimensions, then any variations in composition which lower the free energy of the system must lower the energy required to pack molecules in the cylinder. The proposed cylinder, though not of course stable in the thermodynamic sense, is nonetheless of a geometry which does not suggest high free energies and is thus stable in the biological sense.

4.4. The Cytoplasmic Annulus

We wish to be cautious in interpreting images of the dense mottled layer, regarded here as consisting of the cytoplasmic annulus (DE in Fig. 19 *A*) together with non-demarcated inner and outer regions which are positively-stained layers of head groups belonging to the outer half of the proposed desmotubule bilayer (CD) and to the head group portion of the plasma membrane bilayer (EF). The diagrams used (Figs. 19 *A* and 20) depict an arrangement of 9 lucent particles. There are two reasons for this choice. Firstly, some Markham rotations (not illustrated) gave reinforcements at this number. Secondly, lucent "particles" that could be measured directly from micrographs averaged 4.5 nm for their diameter in the radial direction of the cross-sectioned plasmodesma (Tab. 1, DE): 9 "particles" with circular profile of this diameter fit neatly into the available space with intervening radial gaps 1 nm wide. However, actual images (*e.g.*, Figs. 10–15) by no means justify the clarity of the diagrams. Two possibilities that cannot be excluded are that radial spokes are being positively stained so that the lucent spots are not particles but spaces; and that there is variation in the number of spaces or particles (*cf.* especially Figs. 11 and 14). Nevertheless, occasional observations of chains of lucent spots at appropriate locations in grazing longitudinal sections of plasmodesmata (Fig. 4), and the way in which subunits of microtubules become stained by the tannic acid/$FeCl_3$ procedure (Fig. 1), both support the notion that negatively-stained particles lie in the cytoplasmic annulus. Olesen (1980) also reports nine subunits in the neck constriction of *Salsola* plasmodesmata. In addition, the fact that fragments of plasmodesmata can retain their sub-structural components (Fig. 5), as previously noted and discussed (Burgess 1971, see also Robards 1976), suggests that the whole plasmodesma is an assemblage of stably-linked parts.

The cytoplasmic annulus of plasmodesmata in *Azolla* root primordia is more-or-less parallel sided. It does not display the constricted necks and dilated central portion that are common in other material (review by Robards 1976). The desmotubule has no opportunity to dilate and become more obviously membranous with a clear lumen, as seen outside the orifice (Figs. 15–18) and also in the central nodules of some vascular cells (Wooding 1968, Carde 1974). Instead, *Azolla* plasmodesmata throughout their length closely resemble neck constrictions (as imaged at high magnification by Wooding 1968, Robards 1968, 1976, Carde 1974, Brighigna 1974, Olesen 1975, 1978, Evert *et al.* 1977, and Wochok and Clayton 1976). One reason for favouring a model which the desmotubule has an open lumen was that these images of neck constrictions give the impression that the cytoplasmic annulus is closed – hence if plasmodesmatal transport is to occur, it must be *via* the desmotubule (Olesen 1975, Robards 1976). However, this inference follows only if it is held that the dark staining zone immediately within the plasma membrane bilayer is the wall of the desmotubule, as in the Robards model. If, as held in the present work, the

particulate layer is in the cytoplasmic annulus and the desmotubule has a narrower external radius, then the inference is merely that the cytoplasmic annulus is partially occluded. Implications for symplastic transport are summarised below.

4.5. Implications for Symplastic Transport

The position adopted here lies between two extreme views – on the one hand that the desmotubule is open and the cytoplasmic annulus closed at the neck constrictions; on the other that the desmotubule is closed and the cytoplasmic annulus open. The observations on *Azolla* indicate that the desmotubule has an extremely narrow lumen of cross sectional area equivalent to only a few water molecules packed around lipid head groups, and that the cytoplasmic annulus is partially occluded.

There never has been any evidence that the desmotubule functions in symplastic transport, although the possibility has been the subject of much discussion (*e.g.*, Robards 1976, Gunning and Robards 1976). Indeed when the lumen of the ER is stained or impregnated, the electron density either vanishes or is attenuated in the desmotubule to approximately the dimensions of the central rod (Hawes *et al.* 1981, Hepler 1982 and references therein). There is no obvious reason why this should happen if the ER is continuous from cell to cell *via* open desmotubules.

Restriction of symplastic transport to the cytosol compartment means that plants and animals are similar in this respect. In gap junctions the constituent "connexons" are open to the cytosol, their pores being about 2 nm in diameter, *i.e.*, of cross-sectional area about 3.1 nm^2 (see Loewenstein and Rose 1978). This pore size correlates with a molecular weight exclusion limit in the range 800 (mammalian cells – Flagg-Newton *et al.* 1979) to 1,700 (insect salivary gland – Simpson *et al.* 1977). In view of uncertainty regarding details of the cytoplasmic annulus (preceding section) it would be premature to make over-precise predictions, but in the idealised diagrams of Figs. 19*A* and 20, the cross-sectional area of the inter-particle spaces is in the range 2.6 3.6 nm^2, depending upon assumptions about how close together the particles lie. Accordingly it is conceivable that the molecular weight exclusion limit for plasmodesmata may not be very different from that for gap junctions. The possible effects of partial occlusion of the cytoplasmic annulus on electrical coupling and plasmodesmatal resistances in *Azolla* are discussed in an accompanying paper (Overall and Gunning 1982). There is considerable variation between plasmodesmata from different sources and no claim is made that the above implications apply to all. Clearly none of the models caters for the movement of virus particles, which must be set aside as a special case (Gunning and Robards 1976).

Two final points that should be raised in the present context concern the possibility that symplastic transport is subject to regulation, and the *raison d'etre* for the desmotubule if it is in fact not a tubule. With regard to the first question, if the pore sizes are indeed as small as seems possible, then there are opportunities for regulatory mechanisms whose operation could not be detected by methods of electron microscopy that have been applied to date. Evidence that plasmodesmata alter in electrical resistance in response to treatment with calcium ionophore is presented elsewhere (Overall and Gunning in preparation). Comparison of Figs. 2 and 3 shows that the ER might restrict access to the cytoplasmic annulus becoming flattened against the plasma membrane near the orifice of the plasmodesma. Whether this happens *in vivo* is not known, but several micrographs showing structures apparently bridging the gap between the two membrane systems were obtained (*e.g.*, Fig. 8). Contractile elements so placed could provide some regulation of transport. Other forms of "sphincter" have been discussed (Evert *et al.* 1977, Olesen 1979, 1980).

As to the *raison d'etre* for an essentially non-tubular desmotubule, the suggestion put forward by Gunning and Robards (1976) still stands, namely that the desmotubule might be a stable and static structure around which some form of valve mechanism could operate to open and close the main pathway of symplastic transport, *i.e.*, the cytoplasmic annulus. There is also the possibility of intercellular transmission of signals by propagation along the continuous membrane surface of the endoplasmic reticulum.

Acknowledgements

J. W. thanks CSIRO for a Post-Doctoral Fellowship and R. L. O. acknowledges receipt of an Australian Commonwealth Post-graduate Research Award.

References

Brighigna, L., 1974: The ultrastructure of plasmodesmata in sucking scale in *Tillandsia*. Caryologia **27**, 369 – 377.

Burgess, J., 1971: Observations on structure and differentiation in plasmodesmata. Protoplasma **73**, 83 – 95.

Burton, P. R., Hinkley, R. E., Pierson, G. B., 1975: Tannic acid-stained microtubules with 12, 13 and 15 protofilaments. J. Cell Biol. **65**, 227 – 233.

CARDE, J. P., 1974: Le tissu de transfert (= cellules de Strasburger) dans les aiguilles du pin maritime (*Pinus pinaster* Ait) II caractères cytochimiques et infrastructuraux de la paroi et des plasmodesmes. J. Microscopie **20**, 51–72.

CARNIE, S. L., ISRAELACHVILI, J. N., PAILTHORPE, B. A., 1979: Lipid packing and transbilayer asymmetries of mixed lipid vesicles. Biochim. biophys. Acta **554**, 340–357.

CRISPEELS, M. J., 1980: The endoplasmic reticulum. In: The Biochemistry of Plants, Vol. 1 (STUMPF, P. K., CONN, E. E., eds.), pp. 389–410. New York: Academic Press.

DONALDSON, R. P., BEEVERS, H., 1977: Lipid composition of organelles from germinating castor bean endosperm. Plant Physiol. **59**, 259–263.

EVERT, R. F., ESCHRICH, W., HEYSER, W., 1977: Distribution and structure of plasmodesmata in mesophyll and bundle-sheath cells of *Zea mays* L. Planta **136**, 77–89.

FUTAESAKU, Y., MIZUHIRA, V., NAKAMURA, H., 1972: A new fixation method using tannic acid for electron microscopy and some observations of biological specimens. Proc. Int. Congr. Histochem. Cytochem. **4**, 155–165.

FLAGG-NEWTON, J., SIMPSON, I., LOEWENSTEIN, W. R., 1979: Permeability of the cell-to-cell membrane channels in mammalian cell junction. Science **205**, 404–407.

GRUEN, D. R. W., 1980: A statistical mechanical model of the lipid bilayer above its phase transition. Biochim. biophys. Acta **595**, 161–183.

– WOLFE, J., 1982: Lateral tensions and pressures in lipid monolayers and membranes. Biochim. biophys. Acta (in press).

GUNNING, B. E. S., HUGHES, J. E., HARDHAM, A. R., 1978: Formative and proliferative divisions, cell differentiation and developmental changes in the meristem of *Azolla* roots. Planta **143**, 121–144.

– ROBARDS, A. W., 1976: Plasmodesmata and symplastic transport. In: Transport and Transfer Processes in Plants (WARDLAW, I. E., PASSIOURA, J., eds.), pp. 15–41. New York: Academic Press.

– STEER, M. W., 1975: Ultrastructure and the biology of plant cells, pp. 312. London: E. Arnold.

HAWES, C. R., JUNIPER, B. E., HORNE, J. C., 1981: Low and high voltage electron microscopy of mitosis and cytokinesis in maize roots. Planta **152**, 397–407.

HEPLER, P. K., 1982: Endoplasmic reticulum in the formation of the cell plate and plasmodesmata. Protoplasma **111**, 121–133.

ISRAELACHVILI, J. N., 1978: The packing of lipids and proteins in membranes. In: Light Transducing Membranes (DEAMER, D., ed.), p. 91. New York: Academic Press.

– MITCHELL, D. J., NINHAM, B. W., 1977: Theory of self-assembly of lipid bilayers and vesicles. Biochim. biophys. Acta **470**, 185–201.

JUNIPER, B. E., LAWTON, J. R., 1979: The effect of caffeine, different fixation regimes and low temperature on microtubules in the cells of higher plants. Planta **145**, 411–416.

LA FOUNTAIN, J. R., ZOBEL, C. R., THOMAS, H. R., CALBREATH, C., 1977: Fixation and staining of f-actin and microfilaments using tannic acid. J. Ultrastruct. Res. **88**, 78–86.

LOEWENSTEIN, W. R., KANNO, Y., SOCOLAR, J., 1978: The cell-to-cell channel. Fed. Proc. **37**, 2645–2650.

– ROSE, B., 1978: Calcium in (junctional) intercellular communication and a thought on its behaviour in intracellular communication. Ann. N.Y. Acad. Sci. **307**, 285–307.

LÓPEZ-SÁEZ, J. F., GIMÉNEZ-MARTÍN, G., RISUEÑO, M. C., 1966: Fine structure of the plasmodesm. Protoplasma **61**, 81–84.

MITCHELL, D. J., NINHAM, B. W., 1981: Micelles, vesicles and microemulsions. J. Chem. Soc., Faraday Trans. 2, **77**, 601–629.

NEHLS, R., SCHAFFNER, G., 1976: Specific negative staining of proteins *in situ* with iron tannin. Cytobiol. **13**, 285–290.

OLESEN, P., 1975: Plasmodesmata between mesophyll and bundle sheath cells in relation to the exchange of C_4-acids. Planta **123**, 199–202.

– 1978: Structure of chloroplast membranes as revealed by natural and experimental fixation with tannic acid: particles in and on a thylakoid membrane. Biochem. Physiol. Pflanzen **172**, 319–342.

– 1979: The neck constriction in plasmodesmata: evidence for a peripheral sphincter-like structure revealed by fixation with tannic acid. Planta **144**, 349–358.

– 1980: A model of a possible sphincter associated with plasmodesmatal neck regions. Europ. J. Cell Biol. **22**, 250.

OVERALL, R. L., GUNNING, B. E. S., 1982: Intercellular communication in *Azolla* roots II. Electrical coupling. Protoplasma **111**, 151–160.

– – 1982: Intercellular communication in the filamentous green alga *Oedogonium*: electrical coupling and ultrastructure of plasmodesmata. In preparation.

PIERSON, G. B., BURTON, P. R., HIMES, R. H., 1979: Wall substructure of microtubules polymerised *in vitro* from tubulin of crayfish nerve cord and fixed with tannic acid. J. Cell Sci. **39**, 89–99.

REISS-HUSSON, F., LUZZATI, V., 1964: The structure of the micellar solution of some amphiphilic compounds in pure water as determined by absolute small angle X-ray scattering techniques. J. phys. Chem. **68**, 3504–3511.

REYNOLDS, E. S., 1963: The use of lead citrate at high pH as an electron-opaque stain in electron microscopy. J. Cell Biol. **17**, 208–212.

ROBARDS, A. W., 1968: A new interpretation of plasmodesmatal ultrastructure. Planta **82**, 200–210.

– 1971: The ultrastructure of plasmodesmata. Protoplasma **72**, 315–323.

– 1976: Plasmodesmata in higher plants. In: Intercellular communication in plants: Studies on plasmodesmata (GUNNING, B. E. S., ROBARDS, A. W., eds.), pp. 15–53. Berlin-Heidelberg-New York: Springer.

SEAGULL, R. W., HEATH, I. B., 1979: The effects of tannic acid on the *in vivo* preservation of microfilaments. European J. Cell Biol. **20**, 184–188.

SEMENOVA, G. A., TAGEEVA, S. V., 1972: Ultrastructural organization of intercellular connections between the plasmodesms of plant cells. Doklady Akad. Nauk SSSR **202**, 1427–1428.

SIMONESCU, N., SIMONESCU, M., 1976: Galloylglucoses of low molecular weight as mordants in electron microscopy. J. Cell Biol. **70**, 608–621.

SIMPSON, I., ROSE, B., LOEWENSTEIN, W. R., 1977: Size limit of molecules permeating the junctional membrane channels. Science **195**, 294–296.

SPURR, A. R., 1969: A low-viscosity epoxy resin embedding medium for electron microscopy. J. Ultrastruct. Res. **26**, 31–43.

SINGER, S. J., NICHOLSON, G. L., 1972: The fluid mosaic model of the structure of cell membranes. Science **175**, 720–731.

TANFORD, C., 1973: The hydrophobic effect, pp. 200. New York: Wiley.

TARDIEU, A., LUZZATI, V., REMAN, F. C., 1973: Structure and polymorphism of the hydrocarbon chains of lipids: a study of lecithin-water phases. J. mol. Biol. **75**, 711–733.

TILNEY, L. G., BRYAN, J., BUSH, D. J., FUJIWARA, K., MOOSEKER, M. S., MURPHY, D. B., SNYDER, D. J., 1973: Microtubules: evidence for 13 protofilaments. J. Cell Biol. **59**, 267–275.

VIAN, B., ROUGIER, M., 1974: Ultrastructure des plasmodesmes après cryoultramicrotomie. J. Microscopie **20**, 307–312.

WICK, S. M., SEAGULL, R. W., OSBORN, M., WEBER, K., GUNNING, B. E. S., 1981: Immunofluorescence microscopy of organized microtubule arrays in structurally stabilized meristematic plant cells. J. Cell Biol. **89**, 685–690.

WOCHOK, Z. S., CLAYTON, D., 1976: Ultrastructure of unique plasmodesmata in *Selaginella wildenowii*. Planta **132**, 313–315.

WOLFE, J., STEPONKUS, P. L., 1981: The stress-strain relation of the plasma membrane of isolated plant protoplasts. Biochim. biophys. Acta **643**, 663–668.

WOODING, F. B. P., 1968: Fine structure of callus phloem in *Pinus pinea*. Planta **83**, 99–110.

ZEE, S.-Y., 1969: The fine structure of differentiating sieve elements of *Vicia faba*. Aust. J. Bot. **17**, 441–456.

Printed in Austria